2019 IEEE International Symposium on Safety, Security, and Rescue Robotics (SSRR)
Würzburg, Germany, September 2-4, 2019

Semi-Automated 3D Registration for Heterogeneous Unmanned Robots Based on Scale Invariant Method

Haris Balta[1], Jasmin Velagić[2], Geert De Cubber[1] and Bruno Siciliano[3]

Abstract— **This paper addresses the problem of 3D registration of outdoor environments combining heterogeneous datasets acquired from unmanned aerial (UAV) and ground (UGV) vehicles. In order to solve this problem, we introduced a novel Scale Invariant Registration Method (SIRM) for semi-automated registration of 3D point clouds. The method is capable of coping with an arbitrary scale difference between the point clouds, without any information about their initial position and orientation. Furthermore, the SIRM does not require having a good initial overlap between two heterogeneous datasets. Our method strikes an elegant balance between the existing fully automated 3D registration systems (which often fail in the case of heterogeneous datasets and harsh outdoor environments) and fully manual registration approaches (which are labour-intensive). The experimental validation of the proposed 3D heterogeneous registration system was performed on large-scale datasets representing unstructured and harsh outdoor environments, demonstrating the potential and benefits of the proposed 3D registration system in real-world environments.**

I. INTRODUCTION

Heterogeneous ground-aerial robot systems are becoming increasingly important due to many advantages provided by merging the capabilities of aerial and ground robots into a single collaborative system [1]. Increasing robustness of these systems through fault tolerance as well as their distributed perception and motion possibilities are essential in complex and difficult safety-critical applications, like search and rescue missions. Therefore, this heterogeneous system can achieve a promising performance and higher quality, acquiring more complete information of the environment versus individual robot. However, each platform imposes some limitations. The ground vehicle can sometimes be incapable of traversing and perceiving the entire environment with limited or even unviewable vantage points. On the other hand, the aerial robot typically has limited payload capacities and mostly operates in a shorter time than the ground vehicle.

The logical step would be to fuse capabilities of these different platforms to overcome the limitations of each single one. The main concern in this field of heterogeneous robotic systems is to combine the strengths of the unmanned aerial and ground vehicles [2], [3], [4]. Different cooperative approaches, where the ground vehicle uses the aerial data to improve traversability analysis and path planning, have been proposed in [5]. In [6], a group of ground robots is guided by an aerial vehicle and a human operator while carrying objects within an industrial area. Although deploying a group of heterogeneous aerial and ground robots has become an important topic, very little research has addressed the issues of fusing the 3D data coming from different robots as well as from different sensors. The problems of registering ground and aerial 3D point clouds are related to the different vantage perspectives of the ground and aerial robots. Another problem is a different spatial resolution obtained by the heterogeneous perception systems with different sensor modalities. In our paper, we used UGV with a lidar and the UAV equipped by a high resolution digital camera. The advantages of using a heterogeneous robotic system in an indoor disaster scenario, within an earthquake-damaged building, have been demonstrated in [7]. A team of aerial and ground vehicles performed a collaborative 3D mapping of the building indoors and provided a degree of their damages.

The problem gets more difficult for a large-scale unstructured outdoor environment. Some preliminary work related to this type of environment has been done in [8] for cooperative mapping missions. They proposed a solution for a global alignment of the aerial and ground point clouds based on the Monte Carlo Localization. Their method requires an overlap between the aerial and ground maps and a 3D structure in the scene. Another limitation is that this method does not converge for a completely flat environment. The validation of this system is mostly done indoors, while for the outdoor validation the registration accuracy is not provided due to the fact that no ground truth was available. Our proposed approach successfully handles the limitations for an overlap between the aerial and ground point clouds and does not depend on any environmental characteristics. It is capable of dealing with a large-scale outdoor environments with high geometrical accuracy, as validated with ground-truth data.

In order to overcome limitations of dealing with 3D data sets from different sensors and different perspectives of the environment, we propose a semi-automated and robust 3D registration approach based on the SIRM method. This method includes a scale adaptation and consistent alignment of two heterogeneous point clouds. It should be underlined that our heterogeneous system is fully independent. While many of the existing approaches are more focused on the collaboration between the aerial and ground robots, our research is related to the data fusion of the cluttered 3D environment. In our approach, the aerial map is generated using a photogrammetric structure from motion approach. The

[1]Haris Balta and Geert De Cubber are with Royal Military Academy, Department of Mechanics, Brussels, Belgium haris.balta@rma.ac.be
[2]Jasmin Velagić is with the Department of Automatic Control and Electronics, Faculty of Electrical Engineering, Sarajevo, Bosnia and Herzegovina jasmin.velagic@etf.unsa.ba
[3]Bruno Siciliano is with the Department of Electrical Engineering and Information Technology, University of Naples Federico II, Napoli, Italy siciliano@unina.it

978-1-7281-0778-3/19/$31.00 ©2019 IEEE

UGV is equipped with a 3D lidar range-finder sensor, and the registration of the single 3D scans into a map is done by our proposed LME-ICP method [9], [10]. Two heterogeneous maps are combined into a consistent global map providing an extended view of the environment. Experimental validation of our proposed method is performed in order to demonstrate a real-world applicability of the proposed 3D registration method within search and rescue missions.

The rest of the paper is organized as follows. Section II describes the proposed SIRM method. The obtained experimental results are presented in Section III. In Section IV the conclusions and directions for the future work are given.

II. PROPOSED HETEROGENEOUS REGISTRATION

The proposed semi-automated 3D registration approach based on the SIRM method is shown in Fig. 1. This method is primarily used to align the UAV and UGV point cloud datasets in order to obtain an accurate registration. Its main parts are initial scaling of point clouds and fine alignment with adaptive scaling. The SIRM method is used to solve the problems of displacement, orientation and scale difference between the point clouds. The proposed approach is based on manually marking at least three corresponding point pairs in both point clouds. The transformation between the point clouds is computed and the SIRM method is performed. Therefore, the SIRM is capable of coping with an arbitrary scale difference between the point clouds, without any information about their initial position and orientation.

Before applying the SIRM, we manually select K_{ps} of corresponding points within the two heterogeneous point clouds, acquired by the UGV and UAV. Let $\boldsymbol{R} = \{\boldsymbol{r}_k\}$ and $\boldsymbol{B} = \{\boldsymbol{b}_k\}$, $k = 1, \ldots, K_p$, be sets of corresponding points in the UGV and the UAV point cloud, respectively, where K_p is the number of points in each point cloud and $K_{ps} \geq 3$. The set $\boldsymbol{R} \in \boldsymbol{M}_{model}$ and $\boldsymbol{B} \in \boldsymbol{P}_{source}$, where $\boldsymbol{M}_{model} = \{\boldsymbol{m}_i\}$, $i = 1, \ldots, M_p$ and $\boldsymbol{P}_{source} = \{\boldsymbol{p}_j\}$, $j = 1, \ldots, N_p$, are respectively the UGV and UAV point clouds. The selection of the corresponding points is based on some recognized landmarks, e.g. edge of a house, roof, etc. It is very important to note that the proposed SIRM method overcomes the error between the selection of the corresponding points of heterogeneous point clouds in a range of few meters. This is shown in Fig. 2, where $K_{ps} = 5$ preselected red points representing the corresponding points within the UGV point cloud. The same number of points are selected within the UAV point cloud, which are blue colored. It is obvious that the UAV point cloud has a larger scale and a translational displacement.

A. Initial scaling of point clouds

After selecting corresponding points, the next step is to determine the initial scale. This step is important because we want to achieve homogeneity of the two point clouds by firstly getting them to a similar scale. The initial scale is computed using the mean distances of all possible connections between the selected points as shown in Fig. 3. We have introduced the following expression for the initial scale:

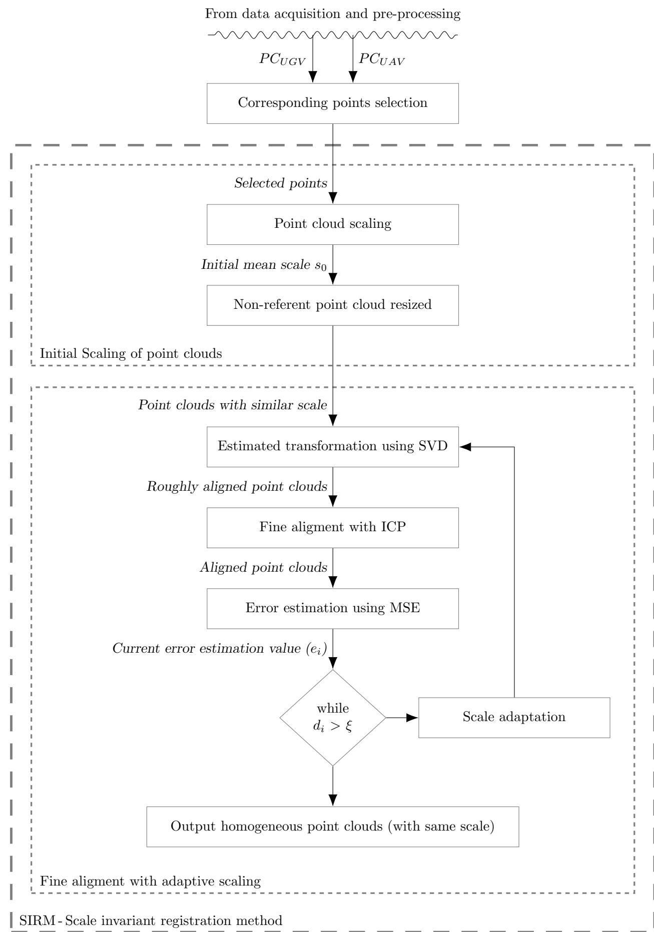

Fig. 1: Proposed Architecture of the Semi-automated 3D registration based on SIRM.

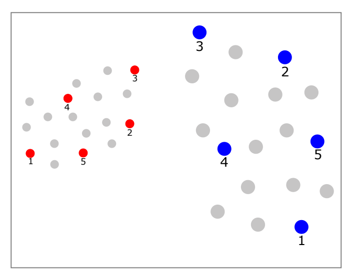

Fig. 2: Illustration of the corresponding point selection.

$$\mathrm{s}_0 = \frac{\sum_{i=1}^{K_{ps}} \sum_{j=i+1}^{K_{ps}} \dfrac{\| \boldsymbol{r}_i - \boldsymbol{r}_j \|}{\| \boldsymbol{b}_i - \boldsymbol{b}_j \|}}{N_{ps}} \tag{1}$$

where $\| \boldsymbol{r}_i - \boldsymbol{r}_j \|$ and $\| \boldsymbol{b}_i - \boldsymbol{b}_j \|$ are the Euclidean distances between two corresponding points in the same point cloud and N_{ps} is number of all possible connections of the preselected points, $N_{ps} = \dfrac{k(k-1)}{2}$.

Once the first initial scale s_0 is computed, we apply its value to resize the UAV (blue) point cloud to be close to the similar scale as the UGV (red) point cloud. In our case, we

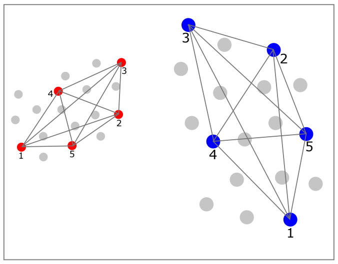

Fig. 3: Illustration of the initial scale estimation process.

rescale the UAV point cloud and use the UGV point cloud as a reference model. Then, we obtain two point clouds with a relative similar scale which allows us to proceed to the second module of the proposed 3D registration approach, the fine alignment with adaptive scaling.

B. Fine Alignment and Adaptive Scaling

After obtaining the similar scale of the two heterogeneous point clouds, a transformation between them is calculated using the singular value decomposition (SVD) [11]. An initial transformation has registered two point clouds relatively close to each other. However, this kind of registration is dependent on the precision of the pre-selected corresponding points and the initial scale computation. Therefore, a good selection of the corresponding points in both point clouds can have a major impact on the scale computation and the final registration results. In order to minimize the error, introduced by the user while selecting the corresponding points, a fine alignment based on ICP method [12] is exploited. In every iteration, the ICP will improve the point clouds alignment. Further improvement is obtained by fine tuning the initial scale computation and transformation registration. For this purpose, the proposed SIRM involves a mechanism for adaptive scale tuning of the mean scale s. It produces the correcting scale factor s_c which is related to the relative difference between two consecutive mean square errors of the two heterogeneous point clouds. The computed value of s_c is then added to the previous mean scale s. After each iteration, the s_c is adjusted and a new transformation between the two points clouds is calculated. The performed transformation is illustrated with black lines in Fig. 4.

In order to evaluate the registration quality, the displacement between the two point clouds in every iteration is computed using a mean squared error (MSE). It is based on the Euclidean distance between the nearest neighbouring

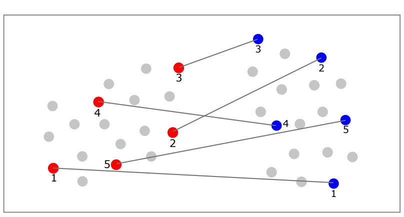

Fig. 4: Fine alignment tuning and registration.

points from the $\boldsymbol{M}_{model}$ and $\boldsymbol{P}_{source}$ point cloud. The mean square error e is expressed by the following equation:

$$e = \frac{\sum_{i=1}^{N} \| \boldsymbol{m}_i - \boldsymbol{p}_i \|^2}{N} \tag{2}$$

In addition, only point pairs with distances shorter than a predefined radius $\boldsymbol{r}$ are taken into account. This radius based error computation is introduced because a significant error is generated by points from the target point cloud which are not captured in the source point cloud, i.e. only the points in the overlapping area with radius r are considered. In each iteration of the adaptive scaling and fine alignment step, we estimated the current error value e_l in accordance to (2). Then, the previous error value e_{l-1} is subtracted from the current obtained error value e_l, where the initial error is set to a large value. The difference between them is given by:

$$d_l = e_l - e_{l-1} \tag{3}$$

The updated mean scale s is computed in each iteration by using the following relation:

$$s_l = s_{l-1} + sc_l \tag{4}$$

where sc_l is correcting scale factor and l is the number of the current iteration. This correcting factor is updated in each iteration based on d_l and error ratio e_l and e_{l-1}:

$$sc_l = d_l \cdot (e_l / e_{l-1}) \tag{5}$$

This adaptive mechanism is proceeded while the error difference d_l becomes larger than the predefined threshold value ξ. The sc_l factor indicates the quality of point clouds alignment with respect to ones in the previous iteration. The smaller values of sc_l mean the better quality of point clouds alignment. This performance index has a smaller value in the case of a simultaneous smaller value of the current e_l and larger value of d_l.

The proposed semi-automated 3D registration obtains relatively accurate initial point clouds alignment when the selected points are corresponding in both point clouds. In this case, the scale adaptive mechanism will very quickly provide accurate point clouds matching with a small mean square error in few iterations. The main power of the SIRM lies in the fast error convergence in heterogeneous point clouds alignment when the selected points from both point clouds are non-corresponding. The initial error alignment is larger than in the first case, but the scale adaptive mechanism will reduce the error in several iterations and produce very precise final point cloud. These statements will be confirmed in Section III. It will be concluded that the scale adaptive mechanism ensures fast convergence of the alignment error and provides very accurate final point cloud. The pseudocode of the proposed semi-automated registration is presented in Algorithm 1.

Algorithm 1 Semi-automated 3D registration method

INPUT $\boldsymbol{PC}_{UGV}$ and $\boldsymbol{PC}_{UAV}$ point clouds
:
OUTPUT Final point cloud $\boldsymbol{PC}_F$
:

```
Select 3 or more corresponding points in point clouds
  Calculation of initial mean scale s_0 between selected points
  Set initial estimation error e_0
  Resize non-reference point cloud using s_0
  do
  |  Point clouds transformation using SVD
  |    Fine alignment using ICP
  |    Error estimation based on MSE scale adaptation
while (d_l > ξ);
return [Final point cloud PC_F]
```

III. EXPERIMENTAL RESULTS

A. Validation Setup

The effectiveness of the proposed approach will be verified for three large scale outdoor environments, entitled Village, Rubble and Dovo. Dimensions of the mapped environments are significantly large (Rubble and Village: $600\,\mathrm{m} \times 200\,\mathrm{m}$; Dovo: $300\,\mathrm{m} \times 250\,\mathrm{m}$). We have performed a qualitative and quantitative evaluation by randomly introducing additional scale, translational and rotational errors. The performance of the proposed method was assessed by two different experiments considering the difference between the selected corresponding points in the heterogeneous point clouds. In the first experimental study (Subsection III-B), the user has visually selected the good Corresponding Points (gCP) in both point clouds. The gCP represents the paired points from both point clouds which are selected from the set of recognized landmarks, e.g. edge of a house, roof, etc., with satisfactory small displacement between them (in cm). The second study (Subsection III-C) considers the situation where the user introduced an uncertainty in the selection of Corresponding Points (uCP) in a range of several meters. It is a significant translation error for the scale and registration.

Each of the considered scenarios has been evaluated on the Dovo dataset, introducing a randomly generated scale and transformation displacement error on the non-referent point cloud, in our case the UAV point cloud. The scale error coefficient $\boldsymbol{k}_{se}$ represents the scale differences between the two point clouds. It was generated up to ten times and it took respectively the following values $\boldsymbol{k}_{se} = [1, 10]$. The transformation displacement error $\boldsymbol{e}_{td} = [e_t, e_r]^T$ represents the displacement error between the two heterogeneous point clouds, as a vector with two components, translational and rotational errors. The range for the translational error was introduced with values of $e_t \in [-50\,\mathrm{m}, +50\,\mathrm{m}]$ for the all Cartesian coordinates (x, y, z). For the rotational error the ϕ, θ, ψ (roll, pitch, yaw) angles were randomly assigned within the range of $e_r \in [-75°, +75°]$ for each axis.

The quality and computational efficiency of the proposed method in both experimental studies for the Dovo dataset are evaluated and the performance analysis is presented. For the qualitative analysis, the following evaluation indicators are used for translation, rotation and scale:

- average error μ for Cartesian coordinates x, y and z and ϕ, θ, ψ angles,
- average Euclidean error ρ for average coordinate errors and angles, minimal and maximal error min and max,
- standard deviation and variance of the error σ and σ^2.

The performance analysis (Subsection III-D) was performed considering all above-mentioned datasets. The last experimental validation was performed with an accurate ground truth reference model, by analysing the accuracy of our registered 3D model with respect to the high accurate geodetic reference model (Subsection III-E).

B. Results with Good Pre-selected Corresponding Points

In this study, we have analysed the case when the user has pre-selected four gCPs in both point clouds of the Dovo dataset. The translation error between the pairs of these points is approximately around $10\,\mathrm{cm}$. The experiment was repeated ten times with different range of error values $\boldsymbol{e}_{td}$ and scale error coefficient $\boldsymbol{k}_{se}$ as in (Subsection III-A). It is obvious from the obtained results (Table I) that the proposed method provides satisfactory matching between the heterogeneous point clouds, regardless of the introduction of large displacement errors for scale, translation and rotation.

In the considered Dovo dataset, the average translational errors are respectively $0.61\,\mathrm{m}$, $0.59\,\mathrm{m}$ and $0.65\,\mathrm{m}$, while the average angular errors are $0.30°$, $0.48°$ and $0.28°$, while the average scale value is 0.04. The computed average Euclidean translational and rotational errors ($1.07\,\mathrm{m}$ and $0.63°$) are relatively low, where the introduced transformation displacement and scale difference error was high. The results obtained for the average Euclidean translational and rotational errors can be treated as a very good outcome of the proposed method. This statement will be confirmed in the Subsection III-D, by showing the quantitative evaluation of our proposed method with respect to a geodetic high precision reference model. In summary, the proposed semi-automated 3D registration method with good pre-selected corresponding points exhibits a promising robustness against large introduced displacement errors for translation and rotation as well as large scale differences. All the qualitative indicators have noticeable small values which guarantees a good matching accuracy of the considered heterogeneous point clouds.

TABLE I: Analytical representation of the results with good pre-selected corresponding points (Dataset: Dovo).

Dataset Dovo							
Par	x [m]	y [m]	z [m]	ϕ [deg]	θ [deg]	ψ [deg]	Scale
μ	0.61	0.59	0.65	0.30	0.48	0.28	0.04
min	0.30	0.01	0.10	0.05	0.00	0.09	0.01
max	1.00	1.42	1.57	0.86	0.89	0.47	0.10
σ	0.24	0.55	0.42	0.26	0.27	0.13	0.03
σ^2	0.06	0.30	0.17	0.07	0.07	0.02	0.00
	Translational Error [m]			Rotation Error [deg]			
ρ	1.07			0.63			

C. Uncertainty in Corresponding Points Selection

This experiment is related to the uncertainty in the process of the manual selection of the corresponding points. It uses the same ten scenarios with the same conditions, as in the previous study, but the error of the pre-selected corresponding points is between $2 - 3\,\mathrm{m}$. That is a remarkable large displacement error in the pre-selected points and it has a significant impact on the accuracy of the heterogeneous point cloud scale and alignment. The obtained values of the considered quantitative indicators using the SIRM are listed in Table II. These values validate the robustness against an uncertainty due to an error in the manual selection of the corresponding points in both heterogeneous point clouds.

The error values of the considered indicators are a bit larger than in the previous experimental study (Table I). However, taking into account the significantly large error value in the selection of the corresponding points, the obtained results are very satisfactory. The SIRM provides well-aligned point clouds, even in the case of large errors in the selection of corresponding points and with large introduced displacement errors for scale, translation and rotation.

D. Performance analysis

For the performance analysis a different number of selected corresponding points in each scenario was used. The minimum number of points used in the Rubble field scenario is four, while the maximum number of points used for the Village scenario was six In addition we used the range for the translational error with values of $\mathrm{e_t} \in [50\,\mathrm{m},\, 250\,\mathrm{m}]$ for all the Cartesian coordinates (x, y, z) and the rotational error the ϕ, θ, ψ (roll, pitch, yaw) angles were assigned within the range of $\mathrm{e_r} \in [-25°,\, +25°]$ for each axis, respectively. The scale error coefficient was set to $k_{se} = 2$. All these errors were introduced for each dataset of the UAV point clouds. Each of the UGV point clouds was set as the reference model while the UAV point clouds were registered on it.

To evaluate the performance of the proposed framework, we use an additional set of parameters: Number of Selected Points (NSP), Computation Time (CT) and Required computer resources (CPU load) for the completion of the specified task. The computational time is the time needed for the proposed SIRM method to register the UAV and UGV datasets into a comprehensive global map. The obtained values of these parameters for our proposed method are listed in Table III. The results indicate that the proposed SIRM method requires between three and a half and ten minutes to register the datasets in both experimental studies, with and without uncertainty in the preselected corresponding points. It is important to note that the SIRM requires this amount of time because of two reasons. The first one is that our datasets have a high density with millions of points in both point clouds. The second reason is that we used the proposed scale adaptive mechanism for fine-tuning of the scale and transformation. Therefore, the proposed adaptive mechanism is running through the iteration in order to minimize the alignment error between the UGV and UAV data set. The CPU load needed for the global map registration is between $27 - 35\,\%$. The hardware we used was PC with an Intel i7-4650 4 Core @ $1.7\,\mathrm{GHZ}$ CPU and $16\,\mathrm{GB}$ of RAM. The resulting global UAV-UGV maps achieved by the proposed SIRM method are shown in Fig. 5.

TABLE II: Obtained results with uncertainty in selection of corresponding points (Dataset: Dovo).

Par	x [m]	y [m]	z [m]	ϕ [deg]	θ [deg]	ψ [deg]	Scale
μ	0.92	0.98	0.69	0.59	0.67	0.54	0.15
min	0.51	0.81	0.13	0.15	0.54	0.13	0.13
max	1.15	1.25	1.25	1.38	1.29	1.01	0.21
σ	0.29	0.19	0.60	0.58	0.34	0.40	0.04
σ^2	0.08	0.04	0.36	0.34	0.11	0.16	0.00
	Translational Error [m]			Rotation Error [deg]			
ρ	1.52			1.04			

Dataset Dovo

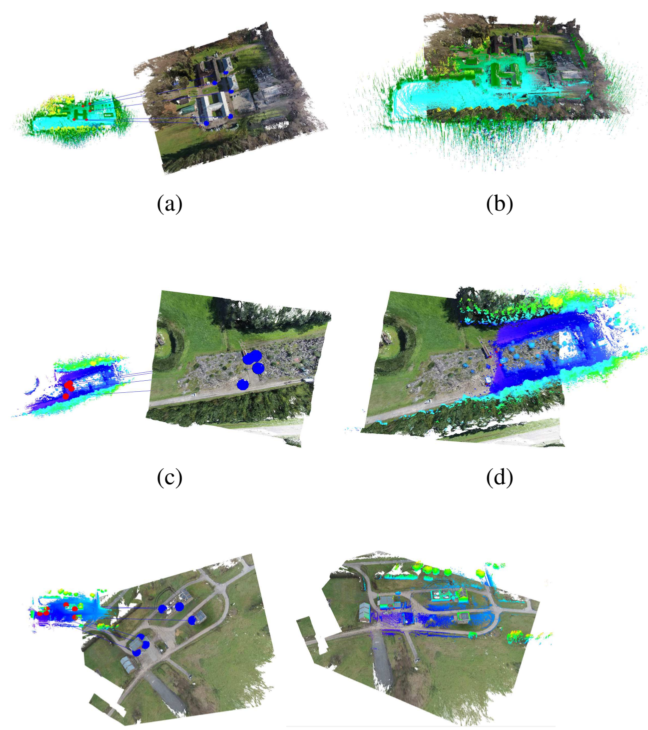

(a) (b) (c) (d) (e) (f)

Fig. 5: Semi-automated 3D registration with pre-selected points and registered UAV-UGV global maps, where a), c) and e) show the manually selected points and the red and blue points which represent the UGV and UAV datasets respectively, whereas b), d) and f) show the final output where the SIRM is applied and the two datasets are registered.

TABLE III: Performance analysis with gCP-good preselected Corresponding Points and uCP-uncertainty in CP selection.

Dataset	NSP	gCP CT (s)	gCP CPU load (%)	uCP CT(s)	uCP CPU load (%)
Dovo	5	223.57	35.05	229.12	36.34
Rubble	4	606.78	26.95	628.23	31.12
Village	6	301.52	32.35	312.41	34.51

In Fig. 5, the UGV point cloud is represented with the elevation (height) map colored with blue and green, while the UAV point cloud is the colorized map. The red dots are the selected corresponding points in the UGV dataset, and the blue dots are the pre-selected corresponding points in the UAV point cloud. Each selected point in one point cloud should have a complementary pair point in the other point cloud. Figs. 5a), c) and e) present the non-registered UGV and UAV point clouds. The obtained maps show the visual representation of all three considered datasets with good pre-selected corresponding points in both point clouds. A very similar result is obtained in the case of an introduced error (about $3\,\mathrm{m}$) while selecting the corresponding points. The reason for that is the small deviation of the scale and alignment errors between the point clouds. Therefore, the visual representation of the resulting maps is not shown. Figs. 5b), d) and f) show the resulting output as a registered UGV-UAV global map. The UAV dataset is scaled and transformed and a good initial alignment is achieved. It can be concluded that the proposed SIRM produces a comprehensive global map satisfying requirements to accurately register datasets.

E. Experimental Study with Ground Truth Reference Model

For the final evaluation we used an accurate ground truth reference model created by a terrestrial geodetic laser system and registered with geodetic precision. We compared the registered UGV-UAV data with the proposed SIRM method with respect to the ground truth using the least square method (LSM). The ground truth and registered maps for the Rubble and Village datasets are shown in Fig. 6.

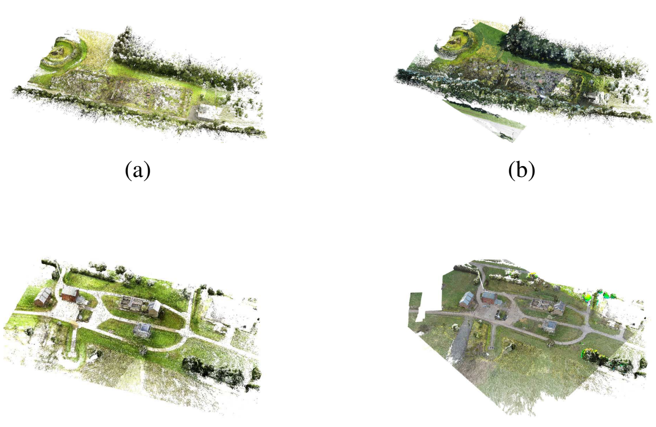

Fig. 6: Comparison of the reference ground truth model (multi-colored) and resulting UGV-UAV datasets. a), b) Rubble and c), d) Village dataset.

The results of the ground truth benchmarking are presented in Fig. 7 and Table IV. Fig. 7 illustrates the point-to-point histograms of the point distribution with respect to their distances. We calculated the distances between points from the ground truth reference model and the co-registered UAV-UGV datasets generated by our proposed SIRM method. It is shown that the proposed SIRM method yielded good results,

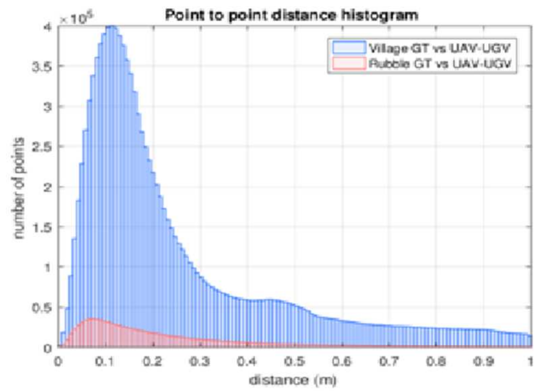

Fig. 7: Point to point error histograms calculated by the distances between points from the ground truth reference model and the registered UAV-UGV map generated by our proposed SIRM method.

where $90\,\%$ of the points are within the distance of $0.51\,\mathrm{m}$ and $0.59\,\mathrm{m}$, for the rubble and village scenarios, respectively. The average error for the rubble scenario is $0.23\,\mathrm{m}$ and for the village scenario $0.25\,\mathrm{m}$ (Table IV).

IV. CONCLUSIONS

In this paper we introduced a novel heterogeneous 3D registration approach for large-scale outdoor environments, which combines heterogeneous datasets acquired from UGV and UAV robots. This approach is based on the proposed SIRM method, which combines a scale invariant method and the ICP algorithm. It performs initial scaling of point clouds as well as an iterative fine alignment with a scale adaptive mechanism. The adaptive mechanism optimizes the scale based on the relative difference between two consecutive mean square errors of the heterogeneous point clouds. This 3D registration is robust to errors in the process of selecting the corresponding pairs of points in both point clouds. The SIRM is capable to cope with an arbitrary scale difference between the point clouds, without any information about their initial position and orientation. Furthermore, it does not require having a good initial overlap between the two heterogeneous UGV and UAV point clouds. The proposed method was validated using large scale datasets, acquired in unstructured outdoor environments. Moreover, a quantitative validation of the reconstruction result was performed by using a reference ground truth data model obtained using a high accuracy geodetic precision measurement system. The obtained results and the performed analyses indicate a good performance of the proposed SIRM method, demonstrating its potential in real world environments.

TABLE IV: Quantitative representation of the point-to-point evaluation for the proposed SIRM method.

	90% of the points are within			
Type	**Rubble**(m)	**Village**(m)	**Rubble Average**(m)	**Village Average**(m)
SIRM	0.51	0.59	0.23	0.25

REFERENCES

[1] M. Garzon,J. Valente, D. Zapata and A. Barrientos, ”An Aerial-Ground Robotic System for Navigation and Obstacle Mapping in Large Outdoor Areas”. Sensors 2013, 13, 1247-1267

[2] M Ani Hsieh, Anthony Cowley, James F Keller, Luiz Chaimowicz, Ben Grocholsky, Vijay Kumar, Camillo J Taylor, Yoichiro Endo, Ronald C Arkin, Boyoon Jung, et al. ”Adaptive teams of autonomous aerial and ground robots for situational awareness”. Journal of Field Robotics, 24(11-12): 9911014, 2007.

[3] H. G. Tanner, ”Switched UAV-UGV Cooperation Scheme for Target Detection,” Proceedings 2007 IEEE International Conference on Robotics and Automation, Roma, 2007, pp. 3457-3462.

[4] B. Grocholsky, J. Keller, V. Kumar, and G. Pappas, ”Cooperative air and ground surveillance,” Robotics Automation Magazine, IEEE, vol. 13, no. 3, pp. 16-25, Sept 2006

[5] A. Stentz, A. Kelly, H. Herman, and P. Rander, ”Integrated air/ground vehicle system for semi-autonomous off-road navigation”, In AUVSIs Symposium on Unmanned Systems, 2002

[6] H. Houssein Chouaib, F. Guerin, F. Guinand, JF. Brethe and H. Pelvillain, ”UAV-UGV Cooperation For Objects Transportation In An Industrial Area”. IEEE International Conference on Industrial Technology, Seville, Spain March 2015

[7] N. Michael, S. Shen, K. Mohta, Y. Mulgaonkar, V. Kumar, K. Nagatani, Y. Okada, S. Kiribayashi, K. Otake, K. Yoshida, K. Ohno, E. Takeuchi, and S. Tadokoro, ”Collaborative mapping of an earthquake-damaged building via ground and aerial robots,” Journal of Field Robotics, vol. 29, no. 5, pp. 832-841, 2012

[8] C. Forster, M. Pizzoli, and D. Scaramuzza, ”Air-ground localization and map augmentation using monocular dense reconstruction”, IEEE International Conference on Intelligent Robots and Systems (IROS), 2013

[9] H. Balta, J. Velagic, G. De Cubber, W. Bosschaerts, B. Siciliano, ”Fast Iterative 3D Mapping for Large-Scale Outdoor Environments with Local Minima Escape Mechanism”, 12TH IFAC SYMPOSIUM ON ROBOT CONTROL - SYROCO 2018, Budapest, Hungary September 2018.

[10] H. Balta, J. Velagic, G. De Cubber, W. Bosschaerts, B. Siciliano, Fast Statistical Outlier Removal Based Method for Large 3D Point Clouds of Outdoor Environments, 12TH IFAC SYMPOSIUM ON ROBOT CONTROL - SYROCO 2018, Budapest, Hungary September 2018.

[11] K. S. Arun, T. S. Huang and S. D. Blostein, ”Least squares fitting of two 3-D point sets,” IEEE Transactions on Pattern Analysis and Machine Intelligence (PAMI), vol. 9, no. 5, pp. 698-700, 1987.

[12] Besl, P. and McKay, N.D, ”A method for registration of 3D shapes”, IEEE Transactions on Pattern Analysis and Machine Intelligence, volume 14, pages 239-256, 2018.